

Blade Fault Localization with the Use of Vibration Signals Through Artificial Neural Network: A Data-Driven Approach

Ngui Wai Keng^{1*}, Mohd Salman Leong², Mohd Ibrahim Shapiai³ and Lim Meng Hee²

¹College of Engineering, Universiti Malaysia Pahang, 26600 UMP, Pahang, Malaysia

²Institute of Noise and Vibration, Universiti Teknologi Malaysia, 54100 UTM, Kuala Lumpur, Malaysia

³Malaysia-Japan Institute of Technology, Universiti Teknologi Malaysia, 54100 UTM, Kuala Lumpur, Malaysia

ABSTRACT

Turbines are significant for extracting energy for petrochemical plants, power generation, and aerospace industries. However, it has been reported that turbine-blade failures are the most common causes of machinery breakdown. Therefore, numerous analyses have been performed to formulate techniques for detecting and classifying the fault of the turbine blade. Nevertheless, the blade fault localization method, performed to locate the faulty parts, is equally important for plant operation and maintenance. Therefore, this study will propose a blade fault localization method centered on time-frequency feature extraction and a machine learning approach. The purpose is to locate the faulty parts of the turbine blade. In addition, experimental research is carried out to simulate various blade faults. It includes blade rubbing, blade parts loss, and twisted blade. An artificial neural network model was developed to localize blade fault through the extracted features with newly proposed and selected features. The classification results indicated that the proposed feature set and feature selection method could be used for blade fault localization. It can be seen from the classification rate for blade faultiness localization.

ARTICLE INFO

Article history:

Received: 17 February 2022

Accepted: 21 June 2022

Published: 19 August 2022

DOI: <https://doi.org/10.47836/pjst.31.1.04>

E-mail addresses:

wkngui@ump.edu.my (Ngui Wai Keng)

salman.leong@gmail.com (Mohd Salman Leong)

md_ibrahim83@utm.my (Mohd Ibrahim Shapiai)

limmenghee@gmail.com (Lim Meng Hee)

*Corresponding author

Keywords: Blade fault, classification, localization

INTRODUCTION

Compressors and turbines are important for extracting energy for petrochemical plants, power generation, and aerospace industries.

The blades of compressors and turbines are the critical parts of their operating system. The failures occurring in compressors and turbines blade result in significant gas turbine damages, catastrophic failure, and financial losses. To illustrate this, Barnard (2006) reported that two catastrophic gas turbine failures account for more than US\$ 25million spent to make up for the production downtime of this equipment.

Moreover, Marsh has testified that turbine and turbine-blade malfunctions continue to be the most typical cause of machinery glitches. It is based on what was experienced by their clients (Marsh, 2016). Therefore, blade fault diagnosis performed on compressors and turbines is essential. The purpose of the diagnosis is to safeguard the safety of this equipment, as well as to prevent significant economic loss. It makes the effective and precise techniques applied for blade fault diagnosis very important.

The singularity discovery approach is the traditional method for blade fault diagnosis, which includes taking a visual depiction of the signal, singularity detection, and the creation of a unique “fingerprint” or “signature.” For example, Peng et al. (2002) applied three distinctive signal processing techniques to determine oil whirl, rotor-to-stator rubbing, and coupling misalignment. The experiment’s results showed that the reassigned wavelet scalogram was a more efficient signal processing method than the frequency spectrum and wavelet scalogram method. In addition, the latest blade fault discovery techniques using time-frequency methods were also anticipated for blade fault diagnosis (Lim & Leong, 2013).

Based on the investigation conducted by Abdelrhman et al. (2014), it was found that wavelet analysis was incapable of separating the frequency components when they were placed close to each other. Two new wavelets were suggested to seek a way out of this problem. According to the findings of the experiment, it was shown that wavelet maps drawn by the suggested new wavelets could not distinguish between the missing blade parts and the defected blade. Besides that, Wang and Chu (2001) recommended a combined wavelet analysis approach and acoustic emission for rubbing fault diagnosis. Chang and Chen (2004) reported that parts in the blade cracks could be localized by applying spatial wavelet analysis. Lim and Ngui (2015) probed the comparison between the effectiveness of the wavelet analysis and vibration spectrum wavelet analysis in diagnosing the blade-related failure. From the experiment, it could be established that both methods are similar for detecting twisted blade conditions. However, a detailed understanding of the vibration spectrum and wavelet map is needed to detect the twisted blade parts.

Overall, most studies mainly focused on detecting blade fault and classifying the fault through the singularity approach. This evaluation approach compares the vibration spectrum or the wavelet map’s amplitudes or patterns. The amplitudes and patterns represent the faulty or healthy condition of a blade. However, there are several challenges and difficulties in deducing the vibration spectrum and wavelet outcomes. Besides, the precision of these

methods depends on the knowledge and individuals' experience in deducing the vibration spectrum and wavelet results.

On the other hand, the artificial intelligence method includes a learning algorithm. With this approach, manual interpretation, which is only subject to the knowledge and the individual's experience, can be relegated. Furthermore, artificial intelligent methods offer automated fault diagnosis (Tiboni et al., 2022; Pang et al., 2020). Previous researchers had also used this method for blade fault diagnosis. The blade features, drawn by vibration signal using frequency domain analysis, were often utilized for blade fault diagnosis. For example, Kuo (1995) studied the occurrence of the wobbly blade, unstable blades, or a blend of these two faults. The defective blades were detected using the aspects drawn from the Fourier analysis as inputs to the ANN. With reference to the investigation, it was clear that the recommended techniques for blade defect classification were workable. Kyriazis et al. (2006) further explored this segment of work. This study investigated the effectiveness of two different models for fusion purposes. Consequently, classification results showed that the information on the recommended combined techniques could be a great instrument utilized for effective blade fault classification. Furthermore, a fault diagnosis method based on ANN was developed. The features extracted from wavelet coefficients as the inputs for ANN were used to classify the blade fault. Consecutively, the proposed techniques were effective for blade fault classification (Ngui et al., 2017). Most of the studies mainly focused on blade fault detection and classification.

For the past few years, numerous studies have been conducted to develop blade fault diagnosis methods. However, there is a limitation in the method for blade fault localization in terms of its ability to locate the blade's faulty parts. Nevertheless, the method for blade fault localization applied to locate the blade's faulty parts is equally important for plant operation and maintenance.

Even though the artificial intelligence method through the machine learning approach was deployed for blade fault diagnosis, its usage was hardly found in the literature. As a result, very few blade fault diagnosis methods are based on machine learning. These methods are developed using the blade features extracted from frequency domain analysis. This process is especially true for blade fault localization. Therefore, this study aims to develop a method that can be utilized for blade fault localization, which is centered on time-frequency feature extraction and machine learning approaches. Several contributions are summarized as follows:

1. The raw vibration signals were analyzed using continuous wavelet transform to extract features as the input for the classifier.
2. A new feature set (blade statistical summation) was proposed to improve the blade fault localization method.
3. A genetic algorithm was used for feature selection.

4. A new blade fault localization method was built based on the extracted features of the recently suggested feature set and feature selection strategy, running on a machine-learning technique.

MATERIALS AND METHODS

Experimental Study

Figure 1 illustrates the blade fault test rig employed to simulate numerous blade fault states. The blade fault test rig, which consisted of multi-stages of the rotor blade, possessed 8, 11, and 13. The vibration signals were measured using two accelerometers (Wilcoxon, model 780A). All accelerometers used in the experiment were calibrated with a Rion VE-10 calibration exciter. The Tacho signal was also captured simultaneously using the optical probe with a reflective tape (Compact Instruments, model VLS-DA1-LSR). Ono Sokki CT-742 Digital Tachometer Display was also used in the experiment to verify the operating speed of the experiment further. A handheld digital tachometer was also used to validate the operating speed of the experiment.

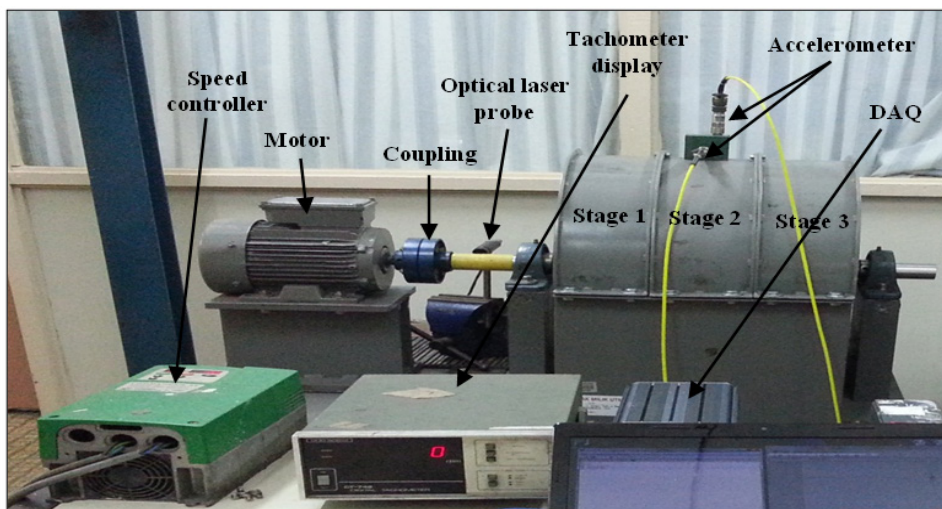


Figure 1. Blade fault test rig

Experiment Procedure

A three-stage blade fault test rig was adopted in this experiment. First, the blade's initial state (no blade defect) was attained before any blade defect was applied to the test rig. Before the blade defect was applied to the test rig, the tacho and vibration signals for the blade's initial state (no blade defect) were attained. These signals were measured at a steady-state sampling rate of 5 kHz with the test rig's rotating speed set to 1200 rpm. With

a sampling rate of 5 kHz, a total of 250 data points were sampled in just one complete cycle of rotation. It is a reasonably fine sampling resolution and is deemed sufficient to prevent any loss of information. Following that, three different blade faults were applied to various stages of the rotor blade test rig.

Then, the corresponding tacho and vibration signals were acquired. Figure 2 presents the three different blade faults simulated on the test rig, which was done by replacing a normal blade with a prefabricated faulty blade. Blade rubbing was performed by substituting one of the normal blades with a prefabricated blade attached to a sheet metal piece. It was done to the prefabricated blade to lengthen the blade's length. Moreover, the rubbing of a single blade was conducted in a state that the blade's edge must simply be in contact with the rotor casing's internal surface. The loss of the blade defect part was presented in the experiment by substituting one of the standard blades with a manufactured one, which went through a partial loss. Finally, a piece of the standard blade was replaced with another and latched onto the rotor disk backward to gain a twisted blade state. Experimental studies for all blade fault conditions were undertaken in a controlled environment. Various measures were undertaken to reduce rotor dynamics instability effect on the experimental results, such as the rotor system's natural frequencies study, rotor balancing, and rotor alignment prior to the experiment. In order to minimize the random error and reduce the noise in the vibration spectra, Synchronous Time Averaging (STA) method was deployed during the signal processing stage. A total of 21 different blades faulted conditions were examined in this study, as illustrated in Table 1. Figure 3 shows the time domain signals for different blade faulted conditions simulated at stage 3.

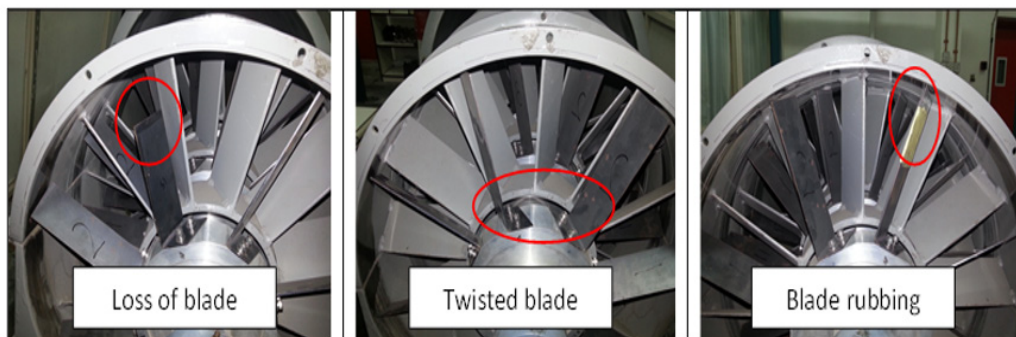
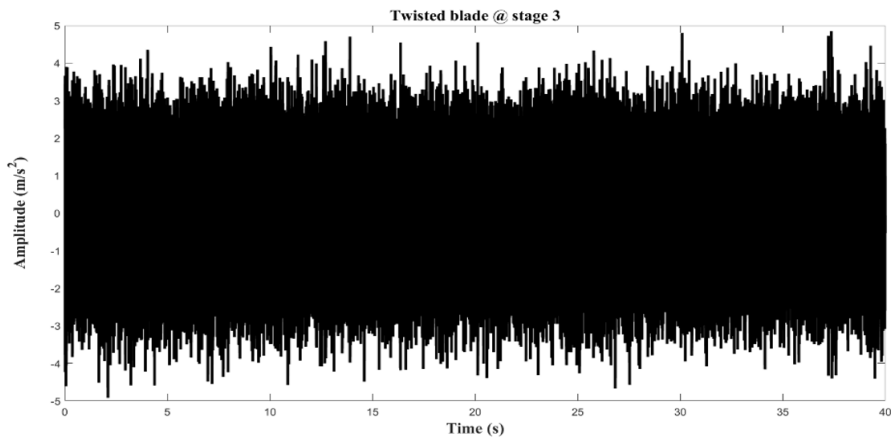


Figure 2. Type of blade faults

Table 1

Blade conditions

Blade condition	Fault location
Loss of blade part	Loss of blade part in stage 1
	Loss of blade part in stage 2
	Loss of blade part in stage 3
	Loss of blade part in stages 1 and 2
	Loss of blade part in stages 1 and 3
	Loss of blade part in stages 2 and 3
	Loss of blade part in stages 1, 2, and 3
Twisted blade	Twisted blade in stage 1
	Twisted blade in stage 2
	Twisted blade in stage 3
	Twisted blade in stages 1 and 2
	Twisted blade in stages 1 and 3
	Twisted blade in stages 2 and 3
	Twisted blade in stages 1, 2, and 3
Blade rubbing	Blade rubbing in stage 1
	Blade rubbing in stage 2
	Blade rubbing in stage 3
	Blade rubbing in stages 1 and 2
	Blade rubbing in stages 1 and 3
	Blade rubbing in stages 2 and 3
	Blade rubbing in stages 1, 2, and 3



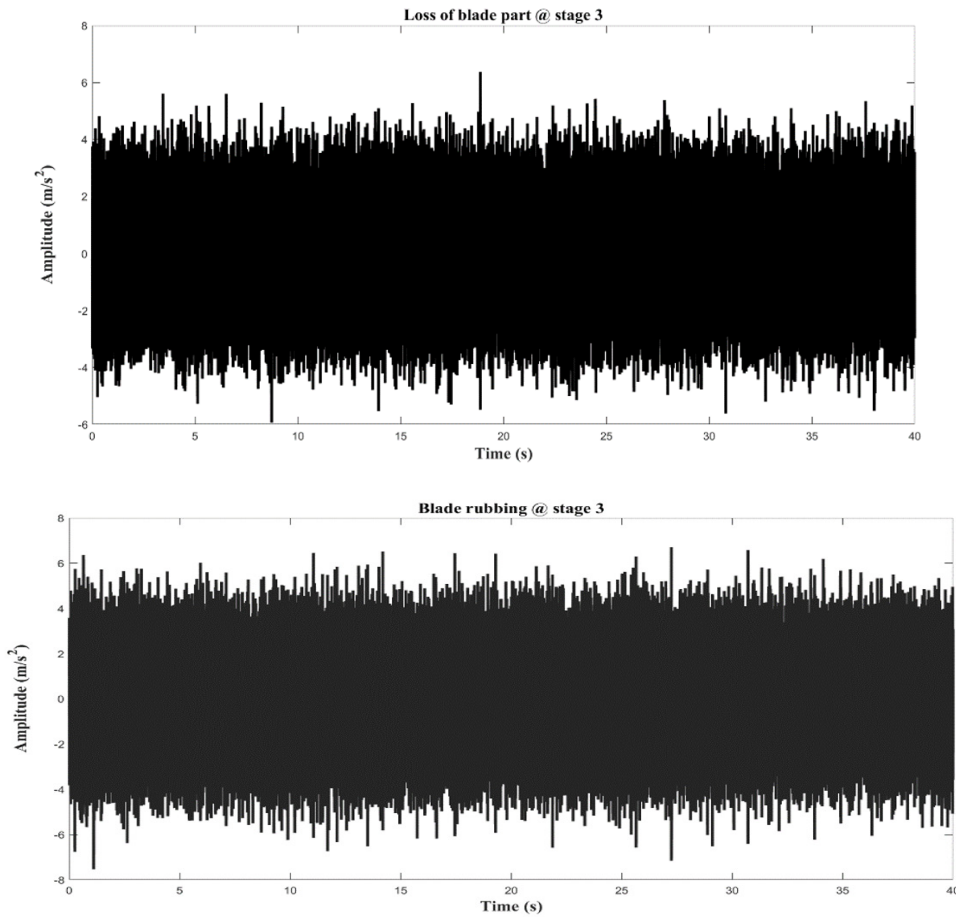


Figure 3. Different blade faulted conditions simulated at stage 3

Feature Extraction

Based on the proposed feature extraction method, statistical features were extracted for blade fault localizations shown in Figure 4. First, the frequencies were filtered apart from the operating frequency and its conforming blade passing frequencies. The operating frequency was 20 Hz, and the blade passing frequencies for stages 1, 2, and 3 were 160 Hz, 220 Hz, and 260 Hz, accordingly, in this experiment. Next, the filtered signal was transformed from acceleration to velocity mode due to the consistent response of the signals to the frequency range of interest. Then, using the tachometer signal as the marker, the signal was divided into smaller segments (one segment represented one complete cycle of rotation). The STA operation was then applied to every 10th vibration to produce the STA signal, representing the average vibration signal produced by one rotation cycle.

Then, each STA signal was used as the input for the continuous wavelet transform to generate the corresponding wavelet coefficients. The Morlet wavelet was preferred for its ability to achieve better performance, indicating machinery fault problems. An amount of 11 statistical parameters, including energy, variance, mean, crest factor, root mean square, kurtosis, standard deviation, central moment, skewness, energy to Shanon entropy ratio, and the Shanon entropy were counted using the wavelet coefficients of the operating frequency and the blade passing frequencies. Consequently, the statistical features were applied to the classifier’s input features.

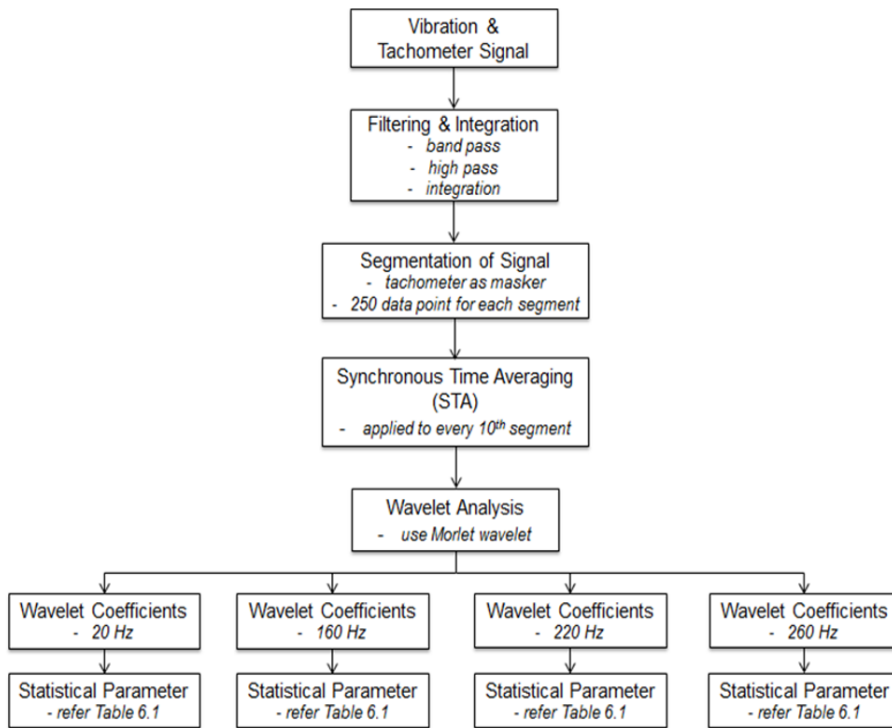


Figure 4. Feature extraction method

Blade Statistical Summation

Besides the statistical features, a new feature set was proposed to acquire more information on blades and produce a better blade fault classification system. This formula went with the following Equation 1:

$$\text{Blade statistical summation} = \sum_{n=1}^N f(x_n) \quad [1]$$

where

$f(x_n)$: statistical value

N : number of statistical value, 4

Using the previously computed statistical features, 22 blade statistical summation were computed. Figure 5 shows the calculation of the blade statistical summation feature.

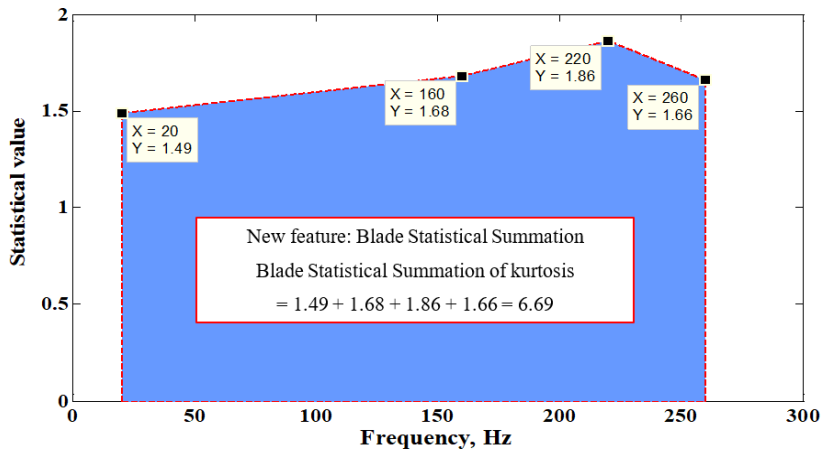


Figure 5. Blade statistical summation

Features Distribution

For each condition of blade fault, a sum of 78 sets of STA signals was extracted from data set A; hence 78 samples were used for feature selection, training, validation, and testing processes. In addition to data set A, 18 sets of STA signals were extracted from data set B (for each condition of blade fault), and all the 18 samples from data set B were used for testing, as presented in Table 2. In summary, from data set A, 1638 samples (21 conditions x 78 samples) were generated from 21 different blade fault conditions, and each condition contributed to 78 samples. As for data set B, 378 samples (21 conditions x 18 samples) were generated as a new testing dataset.

For blade fault localization, two different feature sets were considered inputs in ANN. The first feature set consisted of statistical features extracted from the operating frequency, and the second set considered only the blade statistical summation features.

Table 2

Statistical features and blade statistical summation features

Features	Samples from data set A	Samples from data set B	Total features
Operating frequency (Case A)	1638	378	22
Blade statistical summation (Case B)	1638	378	22

Genetic Algorithm for Feature Selection

Figure 6 shows the feature selection algorithm architecture. The beginning population was generated at random to start the GA algorithm. The process used a binary representation to create chromosomes that signified a subset of the traits. For example, every chromosome's fitness value $F(i)$ is presented as Equation 2:

$$F(i) = CE(i) \quad [2]$$

According to Equation 2, when chromosome i applied a features subset to the training data, $CE(i)$ denoted the classification error. Classification error means the fraction of the total samples wrongly classified by the classifier. Table 3 summarizes the parameters of GA.

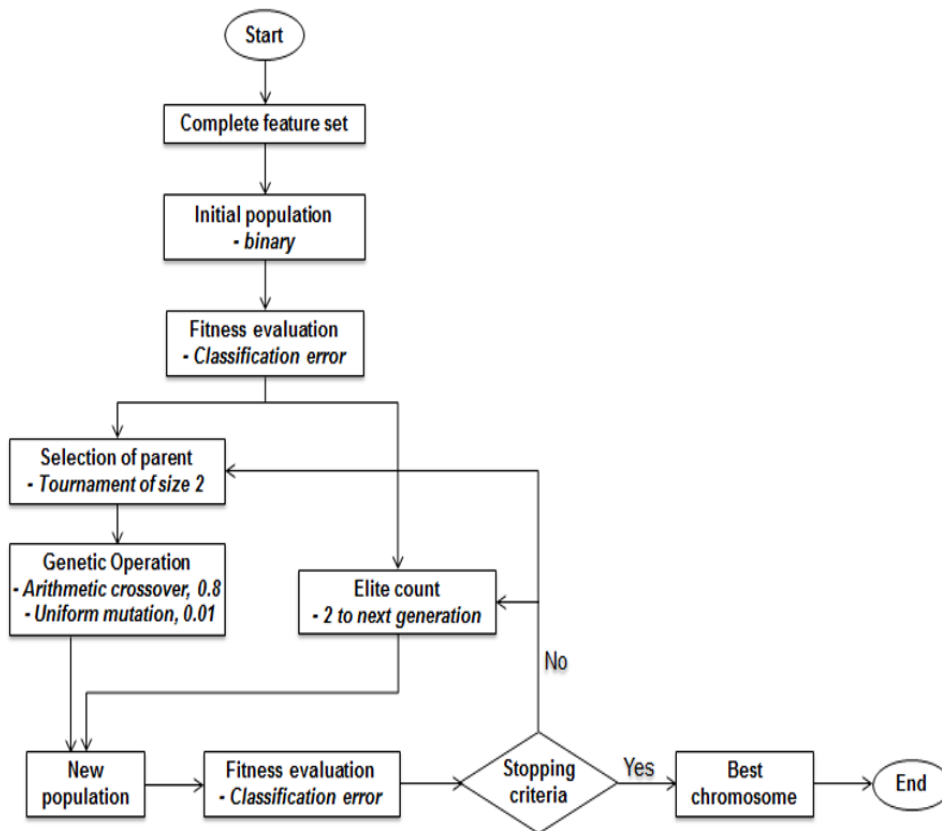


Figure 6. Architecture of feature selection algorithm

Table 3

Parameter for features selection

GA parameter	Selected parameter
Number of generations	100
Size	25
Elite count	2
Selection type	Tournament, size = 2
Mutation type	Uniform, rate = 0.01
Crossover type	Arithmetic, rate = 0.8

ANN Based Blade Faults Localization

A neural network according to a seven-class was created Using the features extracted from the wavelet coefficients and the newly proposed ones. This network aimed to determine the occurrence of blade fault on the parts (stages with blade fault). Seven classes were represented as the parts where blade fault occurred: stage 1, stage 2, stage 3, stages 1 and 2, stages 1 and 3, stages 2 and 3, and stages 1, 2, and 3. This section describes the neural network establishment for blade defect localization. This procedure began by capturing vibration and tacho signals and then was followed by feature selection using the extracted features. The chosen features via GA were then entered into the ANN model for drilling and experimenting. Subsequently, ten-fold cross-validation was performed to train the network with stratified sampling using the selected feature subset. Consequently, the network with the least validation errors was chosen as the last network and administered on the data for testing. Finally, the best subset of chosen statistical feature subsets, as well as of chosen newly proposed feature subsets, are put together and maximized to improve diagnostic performance further and ascertain diagnostic reliability. The purpose of this was to generate the corresponding classification accuracy.

The feed-forward neural network was applied in the present investigation because it performed well when the machinery underwent defects. Also, the number of unseen layers is fixed to two as an increasing number of unseen layers causes overfitting and is time-consuming. Therefore, a neural network with two hidden layers was adequate for mapping the data of arbitrary complexity. Besides that, the number of neurons in the input layer was the same as the number of features. Therefore, the number of neurons in the unseen layer was set at ten. Alternatively, the number of neurons in the output layer was set to seven. Furthermore, the proven ability of the scaled conjugate gradient (trainsig) to solve machinery faults via vibration data was used as the training function in this study. Henceforth, the *tan-sigmoid* function was the switch feature used in each hidden and output layer. Table 4 summarizes the ANN parameters.

Table 4
Parameter of the ANN

Parameter	Selected parameter
Number of neurons in the input layer	Number of selected features
Number of neurons in the hidden layer	10
Number of neurons in the output layer	7
Transfer function	<i>tan-sigmoid</i> function
Training function	Scaled conjugate gradient (<i>trainsig</i>)

For every class, 180 samples (3 kinds of blade fault x 60 samples) from data set A were utilized for training and tested with 108 samples (3 kinds of blade fault x 18 test samples x 2 data sets) from data sets A and B. In this study, two different feature sets (Case A & Case B) were studied as the inputs in ANN for blade fault localization. The first feature set comprised statistical features extracted from the operating frequency. Meanwhile, only the blade statistical summation feature set was considered for the second feature set.

RESULTS AND DISCUSSION

Comparison of Statistical Features and Blade Statistical Summation Features

The newly proposed feature sets and statistical performance for blade fault location were evaluated using two distinctive feature sets as inputs to the ANN. First, the network performance was evaluated using two sets of testing data: A and B. Furthermore, the average accuracy of both testing data sets was represented by their overall accuracy, as shown in Table 5. Based on Table 5, it is apparent that Case A produced the highest overall accuracy in comparison to the two different feature sets. Apart from that, in terms of network generalization, Case A also had the best feature set. Additionally, the newly suggested set of blade statistical sum functions effectively identified blade failures. As a result, the accuracy of the network with the newly proposed feature set was higher than the statistical feature set for the testing data set A. However, this network was less accurate compared to the statistical feature set for the testing data set. Finally, the difference between these two feature sets in terms of the overall accuracy was less than 3%.

Table 5
The performance of statistical and newly proposed feature sets

Case	Testing data A Accuracy, %	Testing data B Accuracy, %	Overall Accuracy, %
Case A	80.95	66.67	73.81
Case B	84.92	57.94	71.43

Feature Selection Using Genetic Algorithm

The performance of the feature selection method using GA is discussed in this section. A neural network was built using similar ANN architecture and sample amounts for training and testing the data. In addition, the network with the least validation error after the 10-fold cross-validation was chosen. 13 and 10 features were selected from Case A and B, respectively. Figures 7 and 8 show the classification error over generations.

The details regarding the ANNs performance, where the features selected by GA for blade fault localization were included, are shown in Table 6. ANN with the selected features from the statistical feature set displayed the best overall accuracy, with a classification rate of 76.72%. It was followed by the proposed feature set's overall accuracy, with a classification rate of 74.07%. The statistical and newly proposed feature sets are effective for blade fault localization.

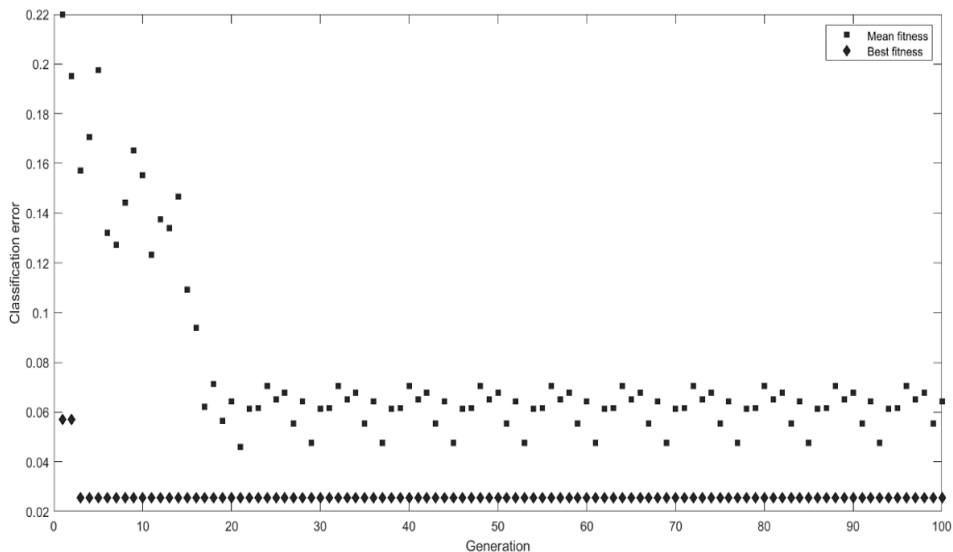


Figure 7. Classification error over generations for Case A

Figure 9 compares the ANNs performance without feature selection and the ANNs performance with feature selection. Based on Figure 9, it can be seen that the ANNs with selected features from GA perform better with fewer features.

According to Table 6 analysis after feature selection, the statistical and newly suggested features are the effective feature subsets in determining blade failure locations. Thus, chosen statistical features and newly suggested features were joined together to improve diagnostic performance further and ascertain diagnostic reliability.

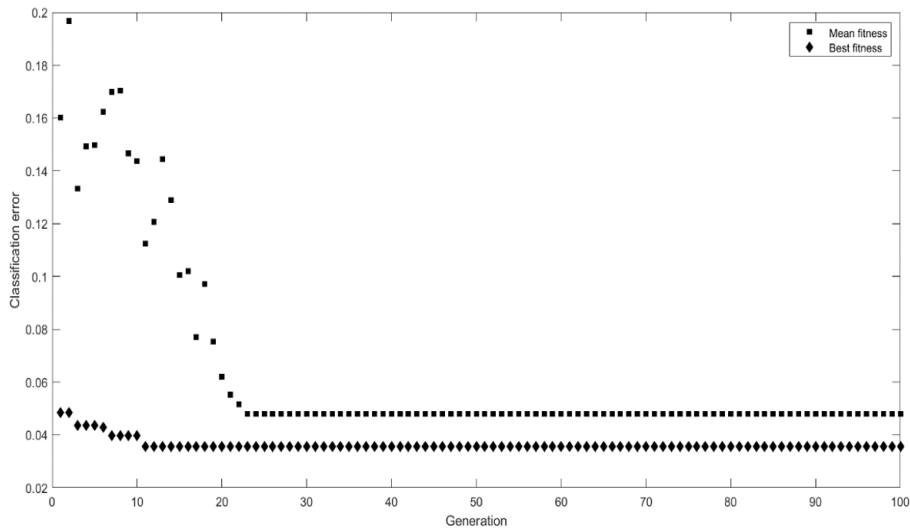


Figure 8. Classification error over generations for Case B

Table 6

Accuracy of different selected feature sets as input for blade fault localization

Feature set	Testing data A Accuracy, %	Testing data B Accuracy, %	Overall Accuracy, %
Statistical feature set	91.80	61.64	76.72
Proposed feature set	89.68	58.47	74.07

The combined feature set was then applied to the proposed algorithm to generate the corresponding classification accuracy. In this instance, 23 features were used as the ANN’s input. On the contrary, the 13 statistical features were from the operating frequency, while the other 10 were the statistical features of the blade. In addition, similar methods elaborated in the previous section were employed to assess the impact of this combined feature set on determining the locations of blade failure. Finally, 10 of the features were removed after the selection feature using GA. Figure 10 shows the classification error over generations.

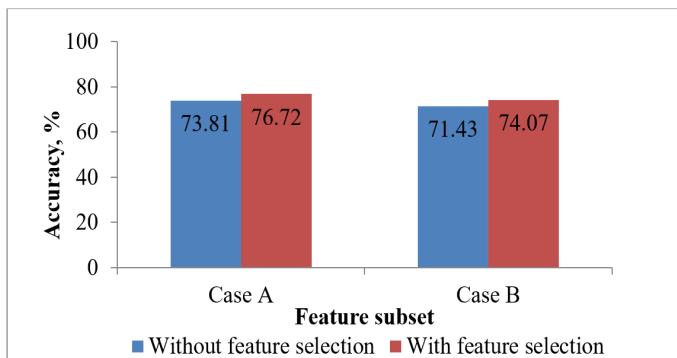


Figure 9. Overall accuracy of blade fault localization for ANNs without feature selection and ANNs with feature selection

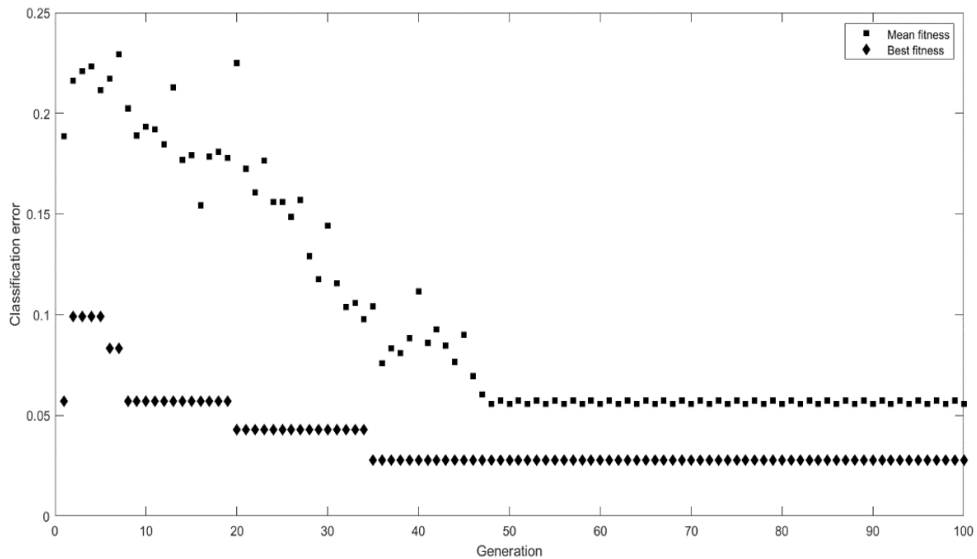


Figure 10. Classification error over generations for the combined feature set

Table 7 illustrates that the combined feature set had produced the utmost testing precision for data set A, testing precision for data set B, and classification precision of all feature sets. Furthermore, not only does the combined feature set after feature selection by GA improve the networks' accuracy, but it also discards unwanted features. Moreover, there was an 11.90% increase in the classification accuracy of testing data set B, from 58.47% to 70.37%. Also, the overall classification accuracy increased between 7% and 9% compared to the overall classification accuracy of ANNs, where only the selected statistical feature subset or newly proposed feature subsets were used as input. Based on the classification results, it was apparent that the extracted features, the proposed new features, and the feature selection method were effective for blade fault localization. Nevertheless, higher accuracy could be attained when the proposed method's statistical features and newly proposed features were applied. Therefore, it can be deduced that the proposed new features and the feature selection method can improve the network generalization capability.

Table 7

Accuracy of selected features of combined feature set for blade fault localization

Feature set	Testing data A Accuracy, %	Testing data B Accuracy, %	Overall Accuracy, %
Statistical feature set	91.80	61.64	76.72
Proposed feature set	89.68	58.47	74.07
Combined feature set	96.56	70.37	83.47

A summary of the classification rate of the ANNs for blade fault localization is shown in Figure 11. In this section, several issues were observed, which are as follows:

1. The features drawn from the operating frequencies were efficient in identifying blade defects.
2. The newly proposed blade statistical summation feature set effectively minimized blade fault.
3. Not only did the features selection method using GA remove unwanted features, but it also enhanced the classification accuracy and network generalization.
4. Combining the statistical and newly proposed features could improve the blade fault localization classification rate.

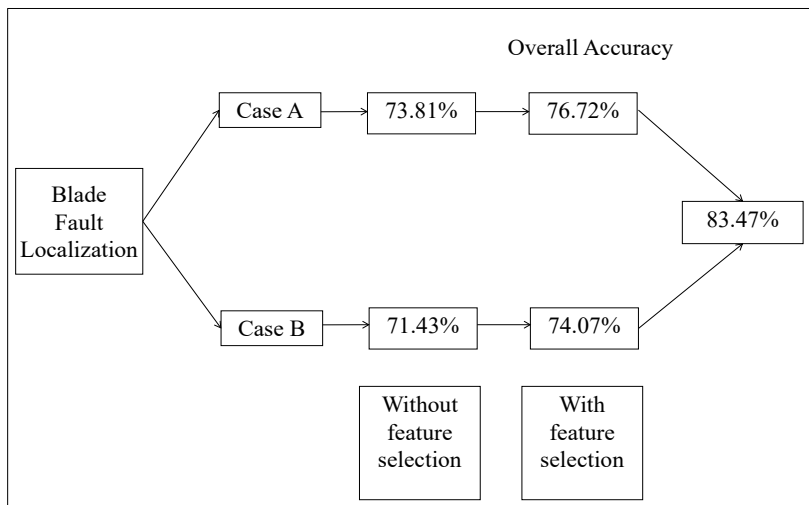


Figure 11. Classification rate

CONCLUSION

The power generation, petrochemical plants, and aerospace industries require turbines and compressors that use blades to generate energy. Hence, the present study produced a new blade defect locating method by adopting the extracted features using the newly recommended feature set and feature selection technique. The experiment found that both feature sets can localize the blade fault position. In addition, the classification results too revealed that the GA-based feature selection method could eliminate unnecessary features and improve classification precision, including network generalization. The selected features of the statistical and newly proposed features were combined to enhance the diagnosis performance further. As a result, there was an increase in the overall classification accuracy, which was between 7% and 9%, compared to neural networks where only the selected statistical features or selected newly proposed features were used as input. In

general, the features extracted by the recent suggested feature set and feature selection technique work well in identifying the location of blade failure. Nonetheless, if the statistical features and proposed new features were utilized, greater exactness could be achieved. As a result, the classification rate for blade fault localization was 83.47%.

ACKNOWLEDGEMENTS

The authors thank the Ministry of Higher Education Malaysia for the financial support provided under the Fundamental Research Grant Scheme (FRGS) No. FRGS/1/2018/TK03/UMP/02/24 grant (University reference RDU190157). The authors also acknowledge the Universiti Malaysia Pahang's support through the Postgraduate Research Grants Scheme (PGRS200303). Additional funding for this research also came from the Institute of Noise and Vibration, Universiti Teknologi Malaysia (RDU192303).

REFERENCES

- Abdelrhman, A. M., Leong, M. S., Hee, L. M., & Hui, K. H. (2014). Vibration analysis of multi stages rotor for blade faults diagnosis. *Advanced Materials Research*, 845, 133-137. <https://doi.org/10.4028/www.scientific.net/AMR.845.133>
- Barnard, I. (2006). Asset management - An insurance perspective. In *Engineering Asset Management* (pp. 44-53). Springer.
- Chang, C. C., & Chen, L. W. (2004). Damage detection of cracked thick rotating blades by a spatial wavelet based approach. *Applied Acoustics*, 65(11), 1095-1111. <https://doi.org/10.1016/j.apacoust.2004.03.006>
- Kuo, R. J. (1995). Intelligent diagnosis for turbine blade faults using artificial neural networks and fuzzy logic. *Engineering Applications of Artificial Intelligence*, 8(1), 25-34. [https://doi.org/10.1016/0952-1976\(94\)00082-X](https://doi.org/10.1016/0952-1976(94)00082-X)
- Kyriazis, A., Aretakis, N., & Mathioudakis, K. (2006). Gas turbine fault diagnosis from fast response data using probabilistic methods and information fusion. In *Turbo Expo: Power for Land, Sea, and Air* (Vol. 42371, pp. 571-579). ASME Publishing.
- Lim, M. H., & Ngui, W. K. (2015, July 12-16). Diagnosis of twisted blade in rotor system. In *22nd International Congress on Sound and Vibration*. Florence, Italy.
- Lim, M. H., & Leong, M. S. (2013). Detection of early faults in rotating machinery based on wavelet analysis. *Advances in Mechanical Engineering*, 2013, Article 625863. <https://doi.org/10.1155/2013/625863>
- Marsh. (2016). *March power and utilities market update*. Marsh LLC. <https://www.marsh.com/pr/en/industries/energy-and-power/insights/marsh-power-and-utilities-market-update-2016.html>
- Ngui, W. K., Leong, M. S., Shapiai, M. I., & Lim, M. H. (2017). Blade fault diagnosis using artificial neural network. *International Journal of Applied Engineering Research*, 12(4), 519-526.
- Pang, S., Yang, X., Zhang, X., & Lin, X. (2020). Fault diagnosis of rotating machinery with ensemble kernel extreme learning machine based on fused multi-domain features. *ISA Transactions*, 98, 320-337. <https://doi.org/10.1016/j.isatra.2019.08.053>

- Peng, Z., Chu, F., & He, Y. (2002). Vibration signal analysis and feature extraction based on reassigned wavelet scalogram. *Journal of Sound and Vibration*, 253(5), 1087-1100. <https://doi.org/10.1006/jsvi.2001.4085>
- Tiboni, M., Remino, C., Bussola, R., & Amici, C. (2022). A Review on vibration-based condition monitoring of rotating machinery. *Applied Sciences*, 12(3), Article 972. <https://doi.org/10.3390/app12030972>
- Wang, Q., & Chu, F. (2001). Experimental determination of the rubbing location by means of acoustic emission and wavelet transform. *Journal of Sound and Vibration*, 248(1), 91-103. <https://doi.org/10.1006/jsvi.2001.3676>